

Numerical Simulation of the Mesoscale Fatigue Crack Propagation in WC/Co under Plane Stress Conditions

Utku Ahmet Özden^{1,a}, Alexander Bezold^{1,b} and Christoph Broeckmann^{1,c}

¹ Institute for Materials Applications in Mechanical Engineering (IWM), RWTH Aachen, Nizzaallee 32, 52072, Germany

^a u.oezden@iwm.rwth-aachen.de, ^b a.bezold@iwm.rwth-aachen.de, ^c c.broeckmann@iwm.rwth-aachen.de

Keywords: WC/Co, Fatigue, Crack propagation, Numerical simulation, XFEM

Abstract. Tungsten carbide-cobalt hardmetals (WC/Co) with high volume percent of WC (75-90 %) are interpenetrating microstructural composites whose two constitutive crystalline phases with widely differing properties (hard, brittle carbides and a tough metallic binder) contributes to one of the most technically successful materials currently in engineering use. Although the metallic binder phase of WC/Co increases the toughness of the composite, on the contrary makes the material susceptible to fatigue failure. Industrial WC/Co components often fail due to long term fatigue.

In this study the fatigue crack evolution of commercial grades were analyzed initially by scanning electron microscope (SEM) and an initial numerical model for fatigue crack propagation was generated using commercial finite element solver Abaqus/Standard with integrated extended finite element method (XFEM) module. The surface propagation of the fatigue crack in SEM can be simulated with plane stress approach. In this respect a basic representative volume element (RVE) of the composite was generated based on SEM analysis. Individual material properties of the two phases were defined and different damage properties were implemented as well for the elastic WC as for the elasto-plastic Co phase. The damage model for the WC phase is based on a generalized linear elastic fracture mechanics (LEFM) principle whereas the Co phase is governed by the continuum damage mechanics (CDM) principle.

From the experimental investigations it was mainly observed that under cyclic loads the fatigue cracks in WC/Co generally initiate from individual carbides or carbide clusters followed by the crack propagation inside the binder phase. Within the framework of this study similar fatigue crack evolution patterns were tried to be obtained with the numerical simulations. Similar to the experimental observations the cracks were initiated from individual carbides and the evolutions of the crack patterns were investigated.

Introduction

The two constitutive crystalline phases of the hardmetal have widely differing properties. Brittle (elastic) phase WC grains contribute to the very high hardness of the material whereas the ductile (elasto-plastic) phase Co contributes to the increased toughness of the material. Although the metallic binder phase increases the toughness of the composite, on the contrary it makes the material susceptible to fatigue failure.

In case of particulate reinforced composites under monotonic loading a common observation of failure mechanism is based on the formation of voids and void coalescence. In this scenario the cracks initially develop by brittle fracture of the individual carbides or carbide clusters which would than propagate further in the binder zone due to the stretching of binder ligaments (plastic straining) eventually leading to the failure of ligaments and formation of voids and void coalescence [1,2]. Similar to those observations, the latest studies conducted in IWM [3] and made by others [4,5] also

indicate that the microcracks leading to the failure of the WC/Co as well originate from large carbides, binderless carbide clusters or from aggregates of WC grains under cyclic loading conditions (Fig 1). However most of the late studies concerning the fatigue crack mechanisms of WC/Co are mainly based on macroscale experimental studies observing fracture toughness (K_{Ic}), the stress intensity factor amplitude (ΔK) and stress ratio (R) variation effects on the fatigue behavior of compositionally varying WC/Co. Those studies as well include the micro-structural observations however does not particularly concentrate on real time fatigue crack propagation observations [4,6,7,8].

Similarly it is possible to observe numerical studies evaluating the micro crack initiation and propagation in WC/Co under monotonic loading conditions in literature [9,10,11]. However, studies evaluating the fatigue crack propagation are not common. The scarcity of numerical simulation of microcrack propagation in WC/Co can be related to the so far experimental complexity and the incapability of the numerical methods in simulating non-predefined crack paths. However latest developments on the experimental techniques, software and computational capabilities make it possible to simulate crack propagation under cyclic loadings. Taking into account such developments current study evaluates the micro fatigue crack propagation in WC/Co with numerical methods based on experimental observations.

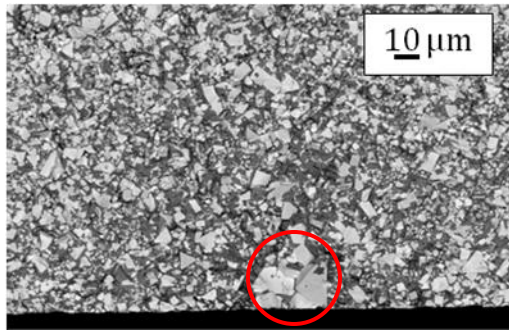


Fig.1. A large carbide cluster observed under SEM as the source of fatigue crack initiation.

Material and Methods

Damage Model for the Inclusion Phase. Within the guidance of the so far conducted studies and observations, a preliminary approach to the micro-mechanical simulation was generated. The principal of this approach was to define separate damage laws for the constitutive phases of the composite. In this respect the WC phase was based on a generalized linear elastic fracture mechanics (LEFM) principle due to the overall elastic behavior of this phase. In LEFM the displacement and the stress near the crack tip can be characterized by the three modes of stress intensity factors (SIF) and the SIF depend on the detailed shape of the solid and the way that it is loaded [12]. Based on the LEFM the growth of the micro cracks inside a carbide grain depends on the critical strain energy release rate and the initial crack length. However observing the initiation of the micro cracks inside the carbide grains was not an objective within the scope of the current study. As indicated before it has already been observed that the cracks initiate due to the cracking of individual carbide grains. Therefore the objective of the current study was to implement a damage model which would realistically predict the direction of the crack growth rather than the initiation of the crack inside the carbide grains. In this regard an initial 3D damage model based on the conventional 3-point bending experimental setup was generated in Abaqus/Standard. The model was composed of 54450 first order enriched linear elastic brick elements. Material properties of WC were based on [13] and defined as isotropic homogeneous.

Two cases were generated depending on the loading scheme in which Case1 = $d/W = 0$ and Case2 = $d/W = 0.5$ (Fig 2a). For each case the initial crack length was progressively increased from 1.5 mm up to 24 mm resulting in 9 individual static simulations and for each simulation the crack growth was not allowed. A unit load was applied to both models and the resultant stress intensity factors for Mode I (K_I) and Mode II (K_{II}) and the crack propagation direction (θ) on set of the crack tip were measured. The out of plane shear displacement effects (K_{III}) were excluded from the measurements since they were not of interest for the current modeling aspects.

In order to validate the simulation results the K_I and K_{II} values were as well calculated analytically. The calculations were based on [14] in which the necessary weight functions and the equations for calculating the K_I and K_{II} values are explicitly defined. In addition the corresponding crack propagation directions (θ) for the analytical calculations were derived from eq.1 [15].

$$\theta = \cos^{-1}\left(\frac{3K_{II}^2 + \sqrt{K_I^4 + 8K_I^2 K_{II}^2}}{K_I^2 + 9K_{II}^2}\right) \quad (1)$$

Similar to the numerical studies the analytical calculations were as well done for both loading cases. For both methods the load was applied on the plane of symmetry (Case1) where the in plane shear displacement equals to zero. In this type of loading the K_{II} and the θ values were both measured and calculated as zero whereas non zero values were measured and calculated for the non-symmetric loading (Case2). The results of both numerical and analytical calculations are plotted in Fig.3. As seen from the figure the calculations for the K_I and K_{II} are in good agreement with minor deviations. On the other hand a much better agreement on the θ values is observed for both cases.

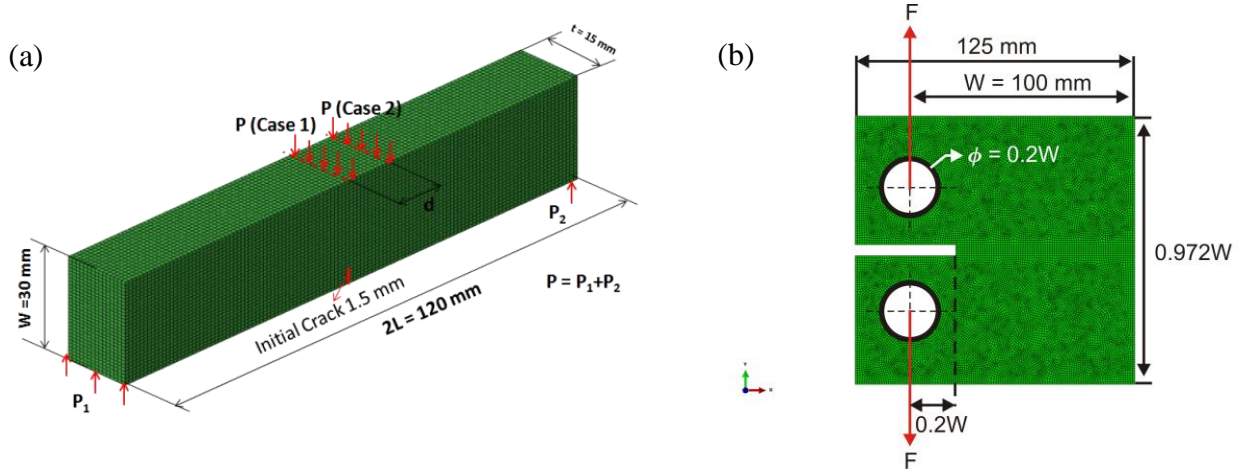


Fig.2. XFEM models based on (a) 3 point bending and (b) Compact tension test specimens.

A quasi static analysis for both loading cases was as well simulated in order to observe and validate the evolution of the crack path. In this regard the same model generated for the static analysis was used (Fig.2a) once again for both loading cases however this time the crack growth was allowed for both loading cases. Definition of damage initiation and damage evolution parameters are required for quasi static XFEM analysis. As indicated before since the individual carbides were already observed to be the source of crack initiation under cyclic loading conditions, a crack initiation criterion was not defined for the model. As an alternative a vertical pre-crack is introduced to the model from which the crack can further propagate. The damage evolution in Abaqus/Standard was based on damage law provided in eq.2.

$$f = \frac{G_{equiv}}{G_{equivC}} \geq 1.0 \quad (2)$$

where G_{equiv} is the equivalent strain energy release rate calculated at a node and the G_{equivC} is the critical equivalent strain energy release rate calculated based on the user specified criteria. For the case study a fracture criterion defined by the eq.3 [16] is selected as the user specified fracture criterion. The criterion is selected since it excludes the Mode III critical strain energy release rate (G_{III}) from the calculations.

$$G_{equivC} = G_{IC} + (G_{IIC} - G_{IC}) \left(\frac{G_{II} + G_{III}}{G_I + G_{II} + G_{III}} \right)^n \quad (3)$$

Since the scope of the current study was to observe the evolution of the crack path rather than validating the fracture toughness of the material, unit values were defined for the Mode I, Mode II critical strain energy release rates (G_{IC} and G_{IIC} respectively) promoting the crack to propagate. The results of the both loading cases were provided in Fig.4. As expected from the static simulation results and analytical calculations in Case1, the crack developed in a vertical path without any deflection whereas in Case2 the crack path deflected from central position towards the applied load.

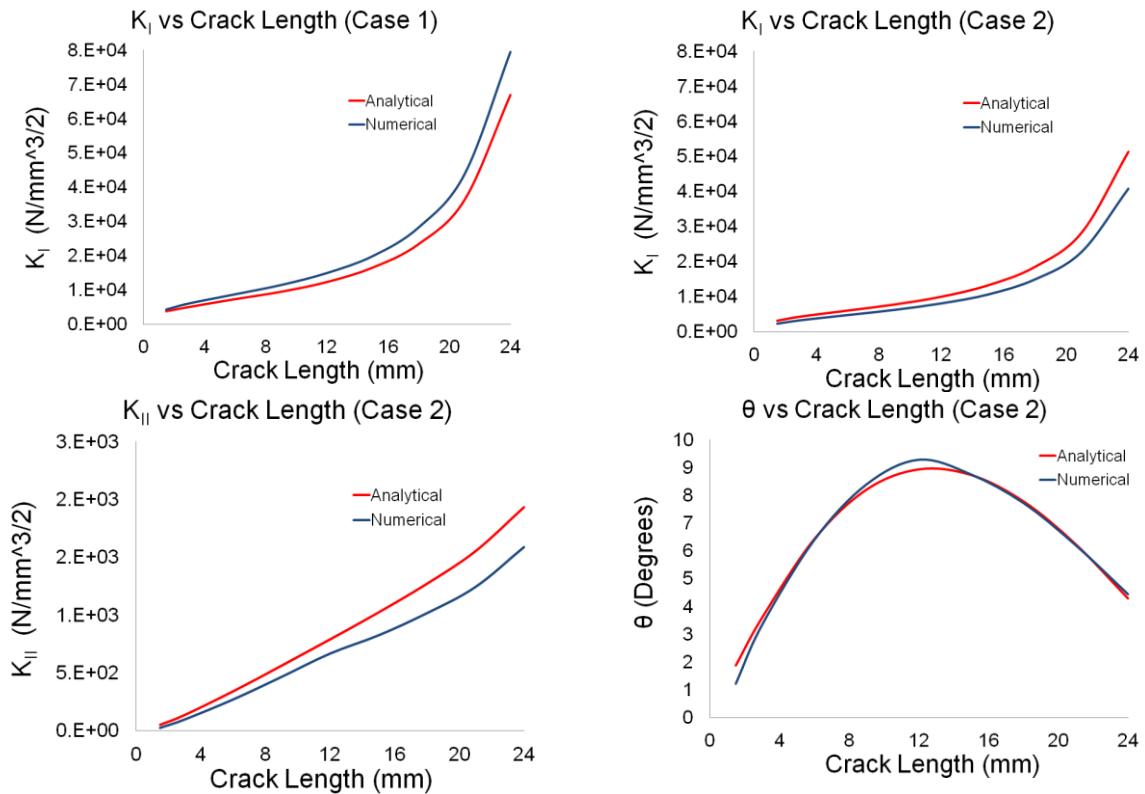


Fig.3. Results of the analytical and numerical calculations for two different loading cases.

Damage Model for the Binder Phase. It is not possible to find a damage model explicitly defining the mechanical behavior of the Co phase in WC/Co under cyclic loading conditions. As indicated before most studies concerning the fatigue behavior of WC/Co are based on empirical relations with

microstructural observations particularly concentrating on the crack origins. However for monotonic loading cases a common approach for explaining the failure mechanism is based on the plastic straining of the binder phase in combination with stress triaxialities [17]. Within the guidance of such observations a damage model for the Co phase was implemented in Abaqus/Standard based on continuum damage mechanics (CDM). In CDM, cyclic loading leads to stress reversals and the accumulation of plastic strains, which in turn cause the initiation and propagation of cracks. The damage model used here for the crack initiation and evolution is based on [18] and is defined by the eq. 4.

$$G_f = \int_{\bar{\varepsilon}_0^{pl}}^{\bar{\varepsilon}_f^{pl}} L \sigma_y d\bar{u}^{pl} \quad (4)$$

where $\bar{\varepsilon}_0^{pl}$, $\bar{\varepsilon}_f^{pl}$, σ_y , L and \bar{u}^{pl} are the equivalent plastic strain at the onset of damage, equivalent plastic strain at failure, yield stress, characteristic element length and the equivalent plastic displacement respectively. As seen from the equation the damage law for the Co phase is based on the accumulation of plastic strains. Another parameter in the equation, characteristic element length is defined since the direction in which the crack occurs is not known in advance. However this parameter does not have significance unless the model contains high aspect ratio elements. Depending on the damage law as soon as the user defined $\bar{\varepsilon}_0^{pl}$ is achieved the damage in the model initiates and the softening response is characterized by the stress-displacement response which is based on the user specified degradation model. Depending on this model the stiffness of the material gradually decreases until the material fully degrades and reaches a final equivalent plastic strain value. This kind of damage approach is particularly practical for the application since the aggressiveness of the fatigue response of the model can be controlled by the user input.

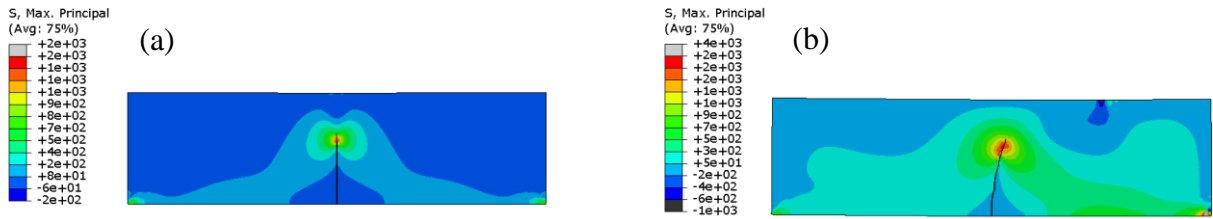


Fig.4. The evolution of the crack path for Case1 (a) and Case2 (b) loading conditions. Color scale: Max. principal stress units in MPa.

In order to test the approach similar to the WC phase an initial experimental model based on a standard notched compact tension specimen was generated. In order benefit from the simulation time a 2D plane stress model composed of 16956 first order elasto plastic quad elements with a particular mesh refinement onset of the crack front was generated. Elastoplastic material properties of Co are based on [13] and defined as isotropic homogeneous. At this point definition of the kinematic hardening parameters is particularly important for the successive accumulation of the plastic strains within the model however due to the lack of explicit data in literature, kinematic hardening parameters of type 316 steel were used for the current model as a substitute. The experimental studies determining those parameters for the Co phase are in the scope of the ongoing

study. An arbitrary critical plastic strain of 0.015 is defined for the damage initiation criteria. On the other hand a linear evolution of the damage variable with plastic displacement is defined for the damage evolution. A force couple exactly symmetric was applied to the holes of the specimen in order to ensure a vertical crack growth. A sinusoidal amplitude having 0.5 Hz. frequency with a ratio of -0.1 was applied to both forces ensuring a non symmetric cyclic loading (ref.Fig.2b). The results of the simulation are represented in Fig.5. As seen from the figure the crack successively propagates until the 17th cycle due to cyclic loading followed by the unstable crack growth leading to eventual failure.

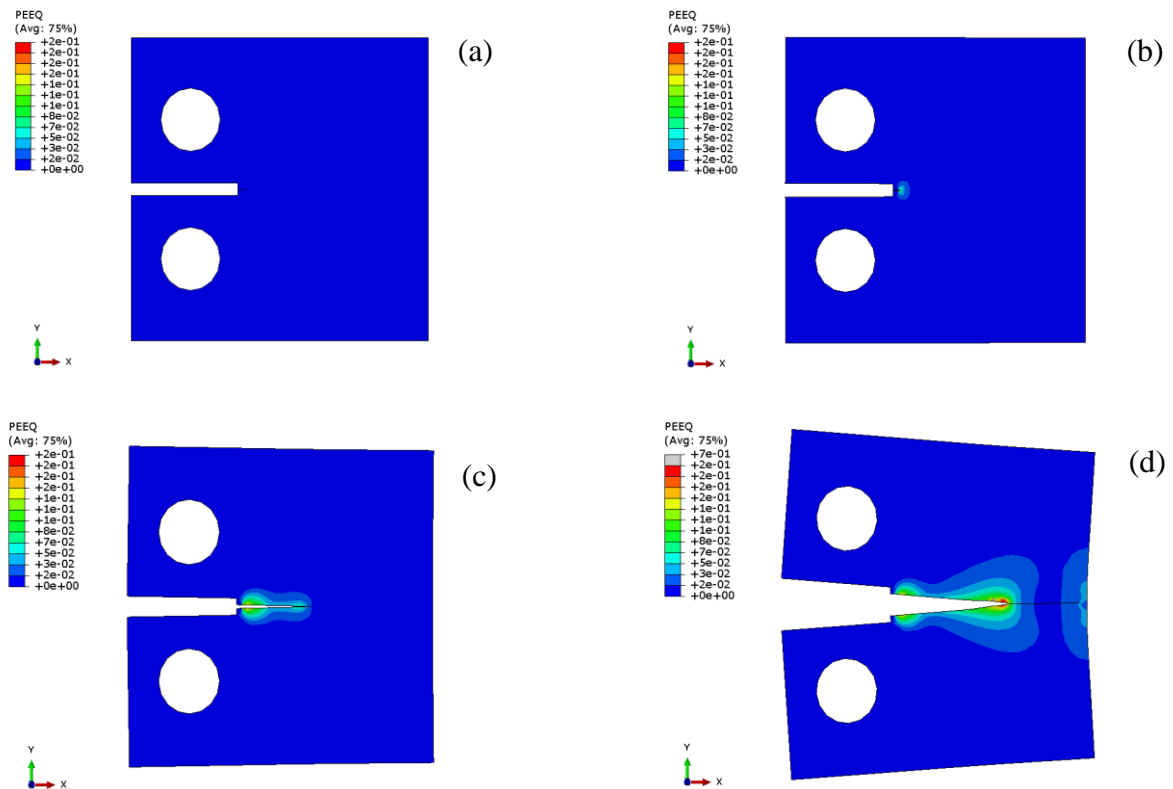


Fig.5. Evolution of the crack path and the successive accumulation of plastic strains in compact tension test specimen under fatigue loading. (a) Load cycle = 0 (b) Load cycle = 5 (c) Load cycle = 17 (d) unstable crack growth. The color scale is fixed to the same range in all images. Color scale: Equivalent plastic strain.

Damage Model for the Composite. The crack propagation studies conducted for the individual phases lead to the generation of the basic damage model for the composite. Depending on the SEM analysis the individual carbides are in the shape of a truncated triangular prism. Although in reality the microstructure of the composite is much more complex with randomly intersecting carbide grains and clusters, for the current damage model a non periodic basic representative volume element (RVE) was generated. The surface crack propagation in the composite can be successfully simulated by the plane stress approach therefore a 2D plane stress model composed of 7190 first order enriched quad elements was generated. Individual material properties and the damage models are defined to the two constitutive phases as before. Once again a constant force was applied to the model and was alternated with the similar type of amplitude used in the damage model for the binder alloy. Finally an initial relatively large crack perpendicular to the loading direction was defined in one of the individual carbide grains in order to initiate the damage inside the material.

As expected the initial crack rapidly propagated on both sides to the edges of the carbide grain by the end of the first cycle followed by the successful propagation inside the binder phase for the ongoing cycles. The propagation of the crack within the binder on both sides continued until the crack surface was fully opened on one edge and the crack meet with the neighbor carbide on the opposite edge (Fig.6). At this point the simulation was terminated since there was no possibility for the crack to further propagate due the lacking of the carbide damage initiation criteria. Currently numerical studies of the ongoing research is based on defining the most suitable crack initiation criteria for the carbide phase so that the crack can further propagate resulting in a fully developed surface damage profile.

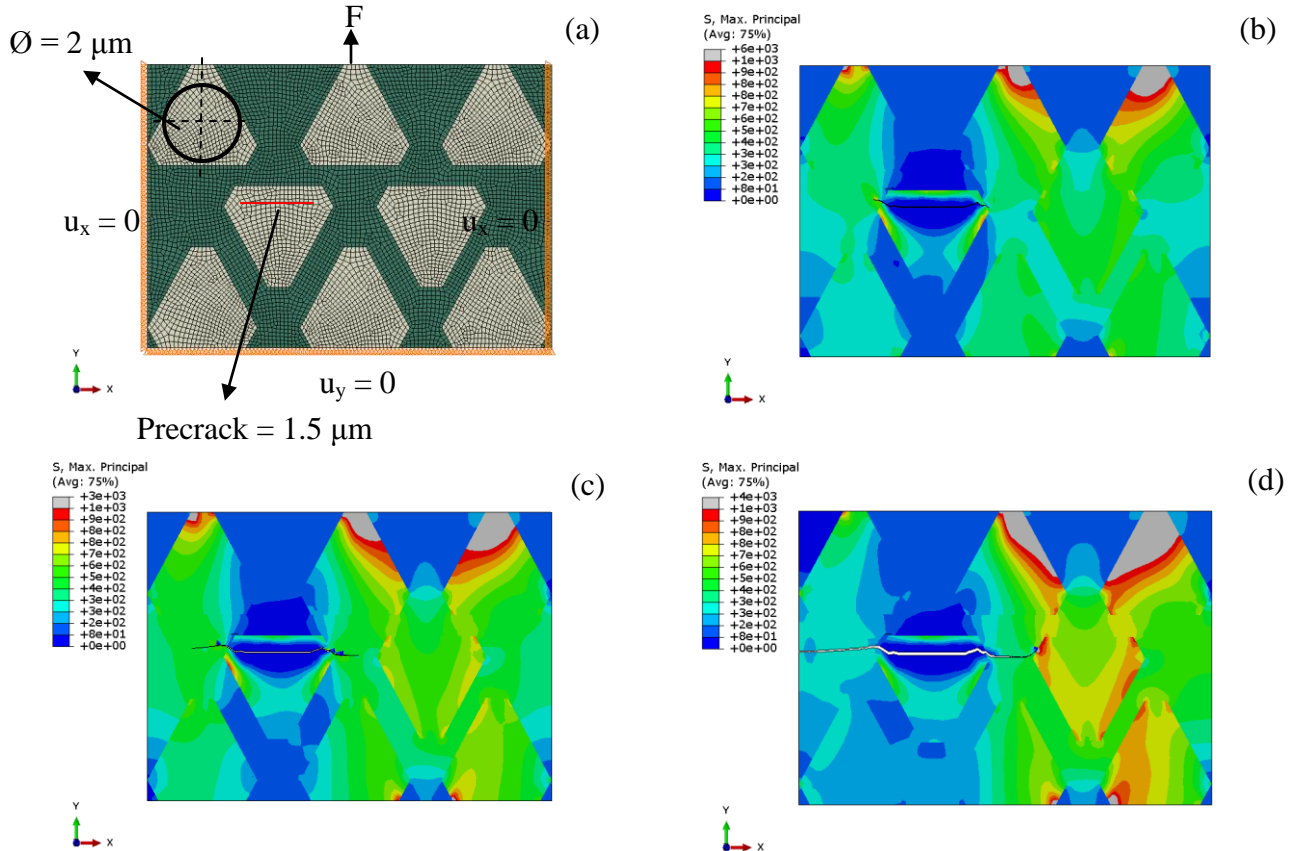


Fig.6. Results of the fatigue simulation for damage model. (a) Model specifications (b) Load cycle =1 (c) Load cycle = 10 (d) Load cycle = 50. The color scale is fixed to the same range in all images. Color scale: Max. principal stress units in MPa.

Conclusion

The aim of the current study was to generate an initial damage model for WC/Co composite based on commercial XFEM code which is capable of simulating fatigue crack propagation based on the experimental observations. In this respect separate damage models were generated for each individual phase, considering their different mechanical nature. A LEFM based damage model was implemented for the WC phase in order to calculate the direction of unstable crack growth depending on the global loading conditions and the results were further validated with the analytical studies.

For the Co phase a different damage model based on CDM was implemented in order to simulate crack propagation under cyclic loading conditions. The damage model was mainly based on the

successive accumulation of plastic strains due to cyclic loading. Due to the lack of explicit data for the kinematic hardening parameters for the current damage model those parameters are currently derived from type 316 steel. Experimental studies on determining the parameters for the Co are within the framework of the future activities.

The final damage model for the WC/Co was based on the combination of two separate damage models defined for individual constitutive phases. The model successively simulates the unstable crack growth within the WC phase and the fatigue induced crack propagation in the binder phase. Initially a crack initiation criterion is not defined for the carbide phase since a pre-crack was introduced to the final damage model however later on the damage model studies reflected the necessity of defining this parameter in order to propagate the crack at the binder-carbide transition.

Overall the main objective of the current study was to investigate the possibility of generating fatigue crack patterns with the numerical methods based on experimental observations in a microstructural WC/Co model. Although many other phenomenons such as the stress triaxility, phase transformation effects and carbide binder decohesion were not taken into account, the current model successively generates crack propagation in WC/Co under cyclic loading conditions.

Acknowledgments

The current study was conducted within the framework of the European Powder Metallurgy Association (EPMA) coordinated SIMU-CRACK I project. In this respect authors would like to acknowledge industrial partners Ceratizit, Hilti, Unimerco, Sandvik Hard Materials and Kennametal Technologies as well as R&D center UPC Barcelona for their ongoing support. EPMA is as well acknowledged for its coordination of the project.

References

- [1] D.F. Quinn, P.J. Connolly, M.A. Howe and P.E. McHugh: *Int. J. Mech. Sci.* Vol. 39 (1997), p.173
- [2] L.L. Mishnaevsky Jr., N. Lippmann, S. Schmauder and P. Gumbsch: *Eng. Fract. Mech.* Vol. 63 (1999), p.395
- [3] S. Keusemann, C. Broeckmann, M. Magin: *Proc. EURO PM Powder Metallurgy Congress & Exhibition; Barcelona, Vol. 1, (2011), p. 209*
- [4] Y. Torres, M. Anglada and L. Llanes: *Int. J. Refract. Met. H.* Vol. 19 (2001), p.341
- [5] T. Klünsner, S. Marsoner, R. Ebner, R. Pippan, J. Glätzle and A. Püschel: *Procedia Eng.* Vol. (2010), p.2001
- [6] Y. Torres, D. Casellas, M. Anglada and L. Llanes: *Int. J. Refract. Met. H.* Vol. 19 (2001), p.27
- [7] L. Llanes, Y. Torres and M. Anglada: *Acta Mater.* Vol. 50 (2002), p.2381
- [8] P.R. Fry and G.G. Garrett: *J. Mater. Sci.* Vol. 23 (1988), p.2325
- [9] H.F. Fischmeister, S. Schmauder and L.S. Sigl: *Mater. Sci. Eng. A.* Vol.105-106 (1988), p.305
- [10] L.S. Sigl and S. Schmauder: *Int. J. Fract.* Vol. 36 (1988), p.305
- [11] P.E. McHugh and P.J. Connolly: *Comp. Mater. Sci.* Vol.27 (2003), p.423
- [12] A.F. Bower in: *Applied Mechanics of Solids*, 2009, CRC Press.
- [13] T. Sadowski and T. Nowicki: *Comp. Mater. Sci.* Vol. 43 (2008), p.235
- [14] T. Fett: *Stress Intensity factors and weight functions for special crack problems (Forschungszentrum Karlsruhe, FZKA 6025 1998).*
- [15] ABAQUS 6.11, ABAQUS Analysis User`s manual 2011.
- [16] M. Benzeggagh and M. Kenane: *Compos. Sci. Technol.* Vol.56 (1996), p.439
- [17] S. Schmauder in: *Encyclopedia of Materials: Science and Technology*, Elsevier Science Ltd., Amsterdam (2001).
- [18] A. Hillerborg, M. Modeer and P.E. Petersson: *Cement. Concrete Res.* Vol.6 (1976), p.773